HHS Public Access

Author manuscript

Biomed Microdevices. Author manuscript; available in PMC 2016 October 03.

Published in final edited form as:

Biomed Microdevices. 2013 April ; 15(2): 221–231. doi:10.1007/s10544-012-9720-1.

Sensitive, microliter PCR with consensus degenerate primers for Epstein Barr virus amplification

Christopher R. Phaneuf,
Department of Mechanical Engineering, Georgia Institute of Technology, Atlanta, GA, USA

Kyudam Oh,
Department of Chemistry, University of Virginia, Charlottesville, VA, USA

Nikita Pak,
Department of Mechanical Engineering, Georgia Institute of Technology, Atlanta, GA, USA

D. Curtis Saunders,
Department of Mechanical Engineering, Georgia Institute of Technology, Atlanta, GA, USA

Christina Conrardy,
Division of Viral Disease, Centers for Disease Control and Prevention, Atlanta, GA, USA

James P. Landers,
Department of Chemistry, University of Virginia, Charlottesville, VA, USA

Suxiang Tong, and
Division of Viral Disease, Centers for Disease Control and Prevention, Atlanta, GA, USA

Craig R. Forest
Department of Mechanical Engineering, Georgia Institute of Technology, Atlanta, GA, USA

Christopher R. Phaneuf: christopher.phaneuf@gatech.edu

Abstract

Sensitive identification of the etiology of viral diseases is key to implementing appropriate prevention and treatment. The gold standard for virus identification is the polymerase chain reaction (PCR), a technique that allows for highly specific and sensitive detection of pathogens by exponentially amplifying a specific region of DNA from as little as a single copy through thermocycling a biochemical cocktail. Today, molecular biology laboratories use commercial instruments that operate in 0.5–2 h/analysis using reaction volumes of 5–50 μL contained within polymer tubes or chambers. Towards reducing this volume and maintaining performance, we present a semi-quantitative, systematic experimental study of how PCR yield is affected by tube/chamber substrate, surface-area-to-volume ratio (SA:V), and passivation methods. We perform PCR experiments using traditional PCR tubes as well as using disposable polymer microchips with 1 μL reaction volumes thermocycled using water baths. We report the first oil encapsulation microfluidic PCR method without fluid flow and its application to the first microfluidic amplification of Epstein Barr virus using consensus degenerate primers, a powerful and broad PCR method to screen for both known and novel members of a viral family. The limit of detection

Correspondence to: Christopher R. Phaneuf, christopher.phaneuf@gatech.edu.

is measured as 140 starting copies of DNA from a starting concentration of 3×10^5 copies/mL, regarded as an accepted sensitivity threshold for diagnostic purposes, and reaction specificity was improved as compared to conventional methods. Also notable, these experiments were conducted with conventional reagent concentrations, rather than commonly spiked enzyme and/or template mixtures. This experimental study of the effects of substrate, SA:V, and passivation, together with sensitive and specific microfluidic PCR with consensus degenerate primers represent advances towards lower cost and higher throughput pathogen screening.

Keywords

Microfluidics; Sensitivity; Virus detection; Polymerase chain reaction; Consensus degenerate; Passivation

1 Introduction

Viral respiratory, gastrointestinal, and encephalitis diseases are often associated with significant morbidity and mortality. Diagnoses of the agents responsible for cases of these diseases in laboratory are difficult because the clinical symptoms of these diseases for different pathogens are often similar or indistinguishable. Traditional detection techniques, including immunoassays, direct fluorescent antigen testing, and viral culturing, are being supplanted by the polymerase chain reaction (PCR), which offers high sensitivity and high specificity in a short turnaround time (Cao et al. 2012). Although conventional PCR-based genomic assays utilizing known pathogen genomic signatures are powerful tools to detect known pathogens, they are incapable of effectively identifying novel emerging pathogens or unsuspected pathogens. Therefore a broad assay for both viral detection and discovery with good sensitivity is needed.

The Centers for Disease Control and Prevention (CDC) use a method for broad diagnosis of viruses by designing specialized primers targeting highly conserved regions across a family and/or genera (Tong et al. 2008; Kaur et al. 2008), known as consensus degenerate hybrid oligonucleotide primer (CODEHOP) PCR (Rose et al. 1998; Rose et al. 2003). Briefly consensus degenerate primers work by observing conserved motifs in the protein sequences of a gene family. From this, a pool of primers is designed with a common 5′ end, known as the consensus clamp that contains a “best guess” sequence for the nucleotides flanking the target motif, and a heterogeneous 3′ end, known as the degenerate core region containing all possible codons for 3–4 amino acids. This methodology not only amplifies nucleic acids from known pathogens but also detects related novel pathogens due to the evolutionary relationships of the organisms.

While PCR has become the gold standard for virus detection, it is more expensive than conventional approaches (Yang and Rothman 2004). Louie et al. (2000) estimates the cost of PCR, when considering reagents, equipment, dedicated space, personnel training, and labor, to be as high as $125 USD per reaction and proportional to reaction volume. In order to reduce PCR costs, the approaches of reducing volume or diluting the reaction mixture are limited by a variety of factors. Conventional PCR tubes are impractical for volumes less than 5 μL due to evaporation, and at these volumes difficulties with sample handling and dilution

has been shown to produce low-quality PCR products (Nakane et al. 2001; Salas-Solano et al. 1998). The development of microfluidic devices for PCR have been proven effective for handling lower volumes and providing faster turnaround times, as detailed in review articles (Zhang et al. 2006; Zhang and Ozdemir 2009). Other advantages of microfluidics can include integration with upstream and downstream sample processing (Easley et al. 2006) and portability for point-of-care applications (Belgrader et al. 2001; Liu et al. 2008). These microchips can be made from a variety of substrates, such as silicon, glass, and, more recently, polymers including poly(methyl methacrylate) (PMMA), cyclic olefin copolymers (COC), polycarbonate (PC), polyester (PE), and polydimethylsiloxane (PDMS); PMMA, PC, COC, and PE are microfluidic substrates that fall in the “glassy polymers” category. Microfluidic device fabrication in polypropylene is rare, though not unheard of (Dahl et al. 2007), because of the challenges of material shaping processes for micro-scale features and bonding. Microchips are fabricated using a wide range of techniques such as chemical etching (Liu et al. 2006; Giordano et al. 2001a), thermoforming (Focke et al. 2010), casting (Yu et al. 2003), and laser etching (Yang et al. 2002). Despite the many advances in the field microfluidics, there are factors limiting largescale adoption such as concerns about usability and sensitivity. In addition, while PCR recipes typically call for a polymerase concentration of 0.02–0.025 U/μL, the recipes for microfluidic PCR frequently require 2–20× more than the conventional polymerase concentration (Angione et al. 2012; Cao et al. 2012; Hua et al. 2010). Within the field of virology, demonstrations of such devices are typically limited to common amplifications at relatively high starting template concentrations (e.g., 0.1–100 ng) (Wang and Burns 2009; Giordano et al. 2001b; Hou et al. 2007). Further, broadrange PCR using consensus degenerate primers have not been demonstrated with microfluidic systems. Ideally, a low-cost microchip produced with simple fabrication would attain sensitivity and specificity comparable to conventional PCR tubes without increased polymerase or template concentration and further be capable of PCR variants such as consensus degenerate PCR.

For proof of concept, we used consensus degenerate primers for pan herpes virus PCR and the Epstein-Barr virus (EBV) as a template. EBV is a double stranded DNA virus belonging to the family *Herpesviridae*. Nearly every human is infected with EBV before adulthood. Infection early in childhood is usually asymptomatic, while delayed primary infection is typically manifest by the signs and symptoms of mononucleosis (Gulley and Tang 2010). After infection, the viral genome is retained for life at low concentration, and presents as illness in higher concentration when the immune system is compromised (Martinez and de Gruijl 2008; Snow and Martinez 2007). Thus, a threshold concentration between low and high viral loads is necessary for diagnostic purposes. There is no consistently published threshold, but one study (Wagner et al. 2001) observed a median high viral load of 32,250 (range 10,150 to 47,450) copies/mL and a low viral load of 7,400 copies/mL. Thus we set a threshold for this work of 3×10^5 copies/mL.

Any viable microfluidic PCR approach must achieve sensitivity and specificity comparable to conventional PCR tubes. As discussed for the EBV virus, sensitivity to a threshold viral load must be defined. Ideal specificity would involve only amplification of the target region for which that particular PCR assay was intended, without amplifying nonspecific products. Here, discernment of the viral target fragments in an electropherogram in the presence of a

noisy human DNA background can serve as a qualitative specificity assessment and comparison to conventional techniques.

One of the most vexing problems encountered when working with low reaction volumes is inhibition due to increased probability of adverse interactions between reagents and inner surfaces of the microfluidic architecture. This is a result of the higher surface-area-to-volume ratio (SA:V), which is the surface area surrounding the reaction divided by the its volume. This problem was acknowledged in early efforts at miniaturization of PCR (Wittwer and Garling 1991; Taylor et al. 1997) and has been explored in the search for the most suitable substrates and effective passivation methods (Giordano et al. 2001a; Panaro et al. 2004; Prakash et al. 2008; Kodzius et al. 2011; Shoffner et al. 1996; Angione et al. 2012; Sweryda-Krawiec et al. 2004; Erill et al. 2003; Christensen et al. 2007; Kolari et al. 2007). It has been shown that the most deleterious factor is adsorption of the polymerase enzyme to the surfaces in contact with the reaction mixture (Erill et al. 2003; Panaro et al. 2004), as well as, in the case of real-time PCR, adsorption of the intercalating dye Sybr Green (Gonzalez et al. 2007). Although some substrates appear to be more inert for PCR purposes, the effects of adsorption appear to occur for most substrates and becomes more pronounced with increasing SA:V. A commonly used reaction volume of 50 μL in a standard polypropylene PCR tube exhibits a SA:V of about 1.3 while microfluidic devices are reported with SA:V more than an order of magnitude higher (Zhang et al. 2006). Despite the recognition of SA:V as a concern for the viability of microfluidic PCR systems, its effects have not been explored systematically. There is a need to determine the threshold in which surface interactions becomes significant so that appropriate substrate choice and passivation considerations can be utilized.

Adsorption of the polymerase enzyme to microscale surfaces has been reported qualitatively (Prakash et al. 2008;) to be a contributing factor in yield reduction at small volumes, and this problem is compounded by the inherent increase in SA:V in microfluidic devices. The specific adsorption of polymerase is commonly explained as a result of hydrophobic interaction between the enzyme and substrate, where hydrophobic substrates will be more likely to adsorb more enzyme (Elbert and Hubbell 1996; Kodzius et al. 2011). Recent studies by Sweryda-Krawiec et al. (2004) and Prakash et al. (2008) have demonstrated adsorption by both hydrophobic and hydrophilic substrates, discounting wettability as a standalone mechanism. Prakash et al. (2008) lists a multitude of possible interactions, including hydrophobicity/hydrophilicity (Koutsopoulos et al. 2004; Orasanu-Gourlay and Bradley 2006; Pancera and Petri 2002), surface free-energy (Noinville et al. 2002), electrostatic attraction/repulsion (Assis 2003; Haynes et al. 1994; Yoon and Garrell 2003), thermodynamics (Haynes and Norde 1995; Norde and Haynes 1995), unique interfacial tension between the protein and adsorbing surface (Beverung et al. 1999), and relationship between protein penetration and steric hindrance from the structure of the protein and adsorbing substrate (Luk et al. 2000; Moskovitz and Srebnik 2005; Sofia et al. 1998). It is worth noting that many authors have suggested that the adsorption mechanisms themselves may not be fully understood (Haynes and Norde 1995; Luk et al. 2000; Sweryda-Krawiec et al. 2004; Yeo et al. 2006).

Several methods have been used to counteract inhibition by adsorption. Dynamic passivation agents (additives to the PCR mixture) such as bovine serum albumen (BSA), polyethylene glycol (PEG), and polyvinylpyrrolidone (PVP) compete with the PCR reagents for adsorption sites on the surfaces of the reaction chamber (Giordano et al. 2001a; Panaro et al. 2004; Kodzius et al. 2011; Shoffner et al. 1996; Angione et al. 2012; Sweryda-Krawiec et al. 2004; Erill et al. 2003; Christensen et al. 2007; Kolari et al. 2007). Further, there is an emerging trend toward droplet microfluidics, in which discrete aqueous volumes (e.g., 100 pL) are encapsulated in oil (Beer et al. 2012; Wang and Burns 2009; Liu et al. 2012) with excellent amplification results. These droplet systems require pneumatic droplet generators and flow cytometers. Ideally, effects and advantages of passivation techniques such as BSA and oil encapsulation could be quantified and/or combined with the simplicity of practical, hand-pipetted volumes (e.g., 1–10 μL) in a disposable polymer chip, without the need for fluid flow to be effective.

We present here experimental characterization of the adverse effects of high SA:V on PCR yield and the efficacy of common methods of passivation to counteract surfacerelated inhibition. These results are applied to the development of a microchip and protocol capable of performing PCR at a 1 μL reaction volume with consensus degenerate primers and standard reagent concentrations to detect EBV with diagnostically relevant sensitivity and specificity, comparable to conventional PCR in a tube.

2 Materials and methods

2.1 PCR reagents

All reactions were prepared from a commercial master mix, AccuPower PCR PreMix (Bioneer, South Korea). This premix consists of a lyophilized pellet of 2.5 U Top DNA polymerase, 250 μM dNTP (dATP, dCTP, dGTP, dTTP), 10 mM Tris–HCl (pH 9.0), 30 mM KCl, 1.5 mM $MgCl_2$, a tracking dye, and a stabilizer.

For testing passivation effects of BSA on various polymers, λ-phage amplification with a 500 bp amplicon was used with a 50 μL volume. For this, both BSA and non-BSA containing reactions were prepared. For the non-BSA reactions, 48 μL of nuclease-free water was added to the premix tube, which was vortexed until the pellet was dissolved and spun down. Next, 1 μL of primer mix, containing 20 μM of the forward (5′-GAT GAG TTC GTG TTC GTA CAA CTG G-3′) and reverse (5′-GGT TAT CGA AAT CAG CCA CAG CGC C-3′) primers (Eurofins MWG Operon, Germany), was added. Purified λ-phage DNA (Affymetrix, Santa Clara, CA) was diluted to 45.8 ng/μL and 1 μL was added to the master mix. For the BSA containing reactions, 38 μL of water and 10 μL of 1 μg/μL BSA (Affymetrix) was used.

For testing passivation effects of mineral oil, the same λ-phage amplification was used. For the non-BSA preparation, 44 μL of water was added to the premix, which was vortexed and spun down. Next, 1 μL of primer mix and 5 μL of λ-phage DNA were added. This mixture was divided into 5 μL aliquots. For the BSA containing reactions, the same protocol was used except the volume of water added was reduced to 29 μL and 15 μL of 1 μg/μL BSA was added to the premix prior to vortexing.

To demonstrate consensus degenerate PCR, we utilized a reaction designed for the *Herpesviridae* family with a 605 bp amplicon. The template DNA was a 4,495 bp plasmid containing an Epstein Barr virus (EBV) genomic fragment and flanking regions of a 3,957 bp vector (Invitrogen, pCR®4-TOPO®). We performed PCR in conventional 0.2 mL PCR tubes at volumes of 5, 3, 2, and 1 μL and our experimental microchips at 1 μL with a variety of template concentrations to assess and compare sensitivity (limit of detection), specificity, and volume limitations. Preparation began by adding 43 μL of water to the premix, which was vortexed and spun down. Next, 1 μL each of 50 μM forward (5′-G(GT)T IGA CTT TGC CAG C(TC)T (GC)TA CCC-3′) and reverse (5′-GGG AGT C(AC)G TGT C(GC)C CGT A(GT)A TGA-3′) primers (supplied by the Centers for Disease Control and Prevention) (Rose et al. 1997) were added, where the parentheticals indicate degenerate base sequences present in the primers. Epstein Barr virus template DNA was prepared with starting concentrations ranging from 1.25×10^{-3}ng/μL (1.4×10^{6} copies/reaction) to extinction in 10× dilution increments to assess sensitivity. For 5, 3, 2, and 1 μL reactions, the mixture was divided into 4.5, 2.5, 1.5, and 0.5 μL aliquots, respectively, and 0.5 μL of DNA was added to each. All volumes were run in conventional tubes in which mineral oil was added to prevent evaporation, keeping the reaction volume confined to the base of the tube. For microchip reactions, 1 μL reaction volumes were used. To assess specificity, 5 ng/μL human DNA was introduced to the reaction mixtures to represent host DNA. A comparison of a 5 μL conventional reaction in a tube and a 1 μL reaction in our microchip was performed, each containing 2.5 ng of host DNA and 1.25 ng of EBV template.

2.2 Thermocycling and detection

Conventional tube reactions were performed in a Bio-Rad MJ Mini thermocycler (Bio-Rad, Hercules, CA, USA). For the λ-phage reaction, thermocycling parameters were as follows: initial denature at 94°C for 2 min, denature at 94°C for 30 s, anneal at 68°C for 30 s, extension at 72°C for 30 s, and final extension at 72°C for 2 min with a total of 30 cycles. Conventional EBV parameters were as follows: initial denature at 94°C for 2 min, denature at 94°C for 15 s, annealing at 48°C for 30 s, extension at 72°C for 30 s, and final extension at 72°C for 7 min with a total of 40 cycles. Microchip reactions were thermocycled using a custom water bath system, where three 1 L volumes of water were maintained at the denaturing, annealing, and extension temperatures and the chips were transferred between them in a stainless steel mesh container. Hold times were extended to ensure thermal equilibrium as follows. For the crucial annealing (e.g., 94°C to 68°C) and extension (e.g., 68°C to 72°C) temperature transitions, 1.5 min of ramping time was determined as more than adequate using a micro-thermocouple (Physitemp, Clifton, NJ, USA) inserted into the reaction chamber. For the less critical denaturing transition (e.g., 72°C to 94°C), 30 s of ramping time was used to quickly reach denaturing without risk of enzyme degradation, bubble formation, or material softening. Thus for the λ-phage reaction, hold times for denature, anneal, and extension were 1, 2, and 2 min, respectively for 30 cycles. Similarly, for the EBV reaction, hold times were 1, 3, and 2 min for 30 cycles.

Following thermocycling, we inspected all chips for air bubble entrainment in the microchambers. We discarded roughly 48 % (19 out of 40) of the chips when air bubbles were visible by naked eye, since preliminary studies showed that PCR was 100 % (15 out of

15) inhibited by their presence, most likely due to the disruption of the oil passivation layer by the bubble, allowing direct contact between the reaction and inhibiting polymer surface.

Electrophoretic detection of PCR products was performed with an Agilent 2100 Bioanalyzer. The reactions were considered “successful” if the signal-to-noise ratio of the electrophoretic peak at the target length was greater than three. For successful reactions, the final concentration of amplicon, or PCR yield (ng/μL), was determined from the Bioanalyzer electropherogram (DNA 1,000 kit for 25–1,000 bp sizing and 0.1–50 ng/μl concentration range). Although real-time detection would have been preferable to provide quantitative PCR results, our methods required endpoint detection, which is considered a semi-quantitative measurement of yield. Therefore, we report ranges of PCR yields for all characterization experiments.

2.3 Surface area-to-volume ratio and substrate characterization

In order to study the effects of SA:V, we performed a set of reactions in volumes of 50 μL in conventional PCR tubes in comparison to a set of higher SA:V by adding segments of polymer capillaries (Paradigm Optics, Vancouver, WA, USA) as shown in Fig. 1. We acquired three different polymer capillaries, poly(methyl methacrylate) (PMMA), polycarbonate (PC), and cyclic olefin copolymer (COC) (Zeonor 1020R, Zeon Chemicals), which are common to polymer microfluidics and compatible with our microchip manufacturing techniques. These capillaries, measuring inner diameter, ID = 500 μm and outer diameter, OD = 750 μm, were diced into segments of length, L = 1 mm and added to the reactions (Fig. 1). These dimensions were used for calculations of surface area to determine the number, N, of capillary segments to add to The reactions for a set of relevant SA:V values, where $SA = N\times\{[\pi(ID+OD)L]+[0.5\pi(OD^2-ID^2)]\}$. Although a 50 μL reaction without added capillary segments has a SA:V of 1.3, representing the polypropylene surface contacting the reaction, this was disregarded in our SA:V calculations, since this contribution is roughly constant for each sample, increasing less than 5% of the total SA:V, due to increased height of the liquid in the tube from displacement by the added capillaries, with the maximum added capillaries. Therefore, effective SA:V values were used to represent the contributions of only the substrates of interest, beginning with 0 for the control reaction, 2.2 for 20 segments, 3.2 for 35 segments, and 5.7 for 63 segments.

The PMMA capillaries were diced using a 40 W CO_2 laser cutter (Trotec Speedy 300) with a custom fixture featuring a vgroove for aligning the capillary. Since the other substrates are incompatible with laser cutting, the capillaries were diced manually using a razor blade. Segments were visually inspected to ensure the capillary was open and a solution of food coloring in water was used to confirm filling of the segments when submerged. Once diced, the capillaries were divided into 20, 35, and 63 segment batches and added to PCR tubes. They were then cleaned by first adding 50 μL of DNase AWAY (Molecular BioProducts), centrifuging and sonicating for 1 h, drying, and repeating the rinse process twice with nuclease-free water. PCR mixtures were pipetted over the capillaries and spun down, ready for thermocycling.

To determine the SA:V of a PCR tube, we added a hemispherical base of radius, R_1 ($SA = 2\pi R_1^2$) to the volume of a frustum, the portion of the conical PCR tube that lies between the

hemisphere and fill height, h, with radius, R_2 ($SA = \pi(R_1+R_2)\sqrt{[(R_1-R_2)^2+h^2]}$). For our PCR tubes (Eppendorf, 951010006), R_1 = 0.92 mm, R_2 = 1.92 mm, h = 6.72 mm. For volumes less than 5 μL, the fill height falls below the top of the hemispherical base and meniscus shape becomes particularly important. For this, the tubes were filled with the low volume, taking care to center it at the base, and the profile was imaged and captured using a microscope. The image was imported into computer-aided design software where the profile was traced and revolved to produce a 3-dimensional representation. Small scaling adjustments were made to ensure the correct total volume and the SA:V values were calculated using the software's measurement features.

2.4 Passivation

The effects of passivation were studied as a function of SA:V using both the capillary segments described above, with SA:V ranging from 0–5.7, as well as polymer microchips with SA:V of 7.0. Using the capillary segments, three different BSA passivation strategies were examined: without BSA, with BSA, and with BSA after overnight (~12 h) incubation. The reagents for these experiments are described in Section 2.1 above, with 0.2 μg/μL as the final BSA concentration. For incubation, samples were immersed in a 30 μL BSA mixture, which was subtracted from the water volume for the recipe described above, allowing the remaining PCR mixture to be simply added to the incubated capillaries. Microchip PCR experiments with BSA were not incubated.

We developed an alternative passivation approach with our microchip involving the use of mineral oil when filling. To encapsulate the aqueous sample in oil analogous to droplet microfluidics, 1.5 μL of mineral oil was first loaded into a pipette tip using an adjustable pipettor. The pipettor volume was increased to 2.5 μL and, after carefully bringing the oil interface to the end of the pipette tip, 1 μL of PCR solution was loaded. The pipettor volume was then increased to 4 μL and the remaining section of the pipette tip was filled with another plug of mineral oil. This volume is loaded into the microchip, aligning the PCR solution to the reaction chamber (Fig. 2). Upon visual observation at 20×, the oil appears to form a smooth boundary between the droplet and chamber walls, suggesting a fully encapsulating layer between them.

2.5 Microchip fabrication

We used micromilling as the ideal fabrication method for glassy polymers as a result of the ability to quickly iterate in the design process as well as the ability to achieve threedimensional geometries with relatively low SA:V compared to the range of dimensions and contour complexity possible with conventional semiconductor and molding-based manufacturing. Micromilling offers minimum feature sizes of 125 μm and produces surface roughness of approximately 350 nm. We chose PMMA for our microchips, which are postage stamp sized disposable cartridges that feature two chambers, each with a pair of filling channels and ports for loading and unloading (Fig. 2). Microchips were fabricated by first dicing a 1.5 mm thick PMMA sheet into 20×12.5 mm blanks by CO_2 laser cutting. Features were machined via micromilling using a high-speed computer numerical control vertical milling machine (Haas Automation, Oxnard, CA, USA), as previously described (Phaneuf and Forest 2010; Pak et al. 2012). Each microchip features two 500 μm wide

chambers with a volume of 1 μL along with 250 μm wide filling channels and 700 μm diameter ports. Using computeraided design software, we determined the SA:V for the chamber to be 7.0. The reaction chambers and filling channels were encapsulated by thermal bonding using a custom tellurium copper fixture heated to 170°C on a hot plate and clamped for 30 min. The microchip was filled using a standard micropipette by first loading a pipette tip with PCR solution, seating the pipette tip on a port, applying gentle force to create a temporary seal, and injecting the sample until the PCR solution is centered within the reaction chamber. Overflow was absorbed with a lint-free wipe and the ports were sealed with a commercial 50 μm thick adhesive film (Sigma-Aldrich, St. Louis, MO, USA). The process is depicted in Fig. 2.

3 Results

3.1 Conventional PCR

We examined the lower limits of volume using conventional tubes by testing volumes of 5, 3, 2, and 1 μL (SA:V = 3.1, 3.8, 4.5, and 5.7, respectively) with serial dilutions of EBV template. One set followed a conventional recipe (Fig. 3(a)) and the other used 0.2 μg/μL BSA for passivation (Fig. 3 (b)). Success rate decreased with decreasing volume and benefited from the addition of BSA. None of the 1 μL reactions were successfully amplified.

3.2 Effects of surface-area-to-volume ratio, substrate, and passivation

From the capillary segment experiments, we measured PCR yield versus SA:V as shown in Fig. 4(a). Overall, the adverse effect of increasing SA:V is apparent in the decreasing yield for each substrate. The COC appears to be the most compatible polymer, with PC displaying slightly lower but not significantly different final concentrations ($p<0.05$ at each SA:V), and PMMA was the weakest performer. We observe an inverse relationship for all materials with increasing SA:V.

We next looked into quantifying the effects resulting from various passivation chemistries, as shown in Fig. 4(b, c). The yield at high SA:V (e.g., >3) is improved and stabilized by the addition of BSA. Incubation further enhances this effect. This stabilization of yield makes PCR viable at SA:V as high as 5.7 for all substrates tested in this work.

We performed a variety of experiments in PMMA microchips to explore the effects of passivation and high SA:V (SA:V = 7.0), as shown in Fig. 5. Relative to a 50 μL control reaction in a conventional PCR tube, we measured the PCR yield in the four combinations with/without BSA (nonincubated) and with/without oil. As before, PMMA at high SA:V (in the microchip) without passivation consistently fails and has a low but consistently detectable yield with BSA. The favorable effect of loading a PCR sample between plugs of mineral oil in a PMMA microchip compared to without oil was significantly different ($p<0.05$). In addition to the benefit of loading with mineral oil compared to without, the exclusion of BSA further improved performance.

3.3 Sensitivity of microfluidic consensus-degenerate PCR

Using the PMMA microchip (volume = 1 μL, SA:V = 7.0) with optimal passivation of oil without BSA, we performed amplifications of EBV template using pan herpes virus consensus degenerate PCR with a serial dilution of template from 0 to 10^6 starting copies to determine the sensitivity of this optimized microfluidic device. The results, with corresponding starting concentration and yield, are shown in Fig. 6. The samples were successfully amplified down to the desired threshold of ~100 starting copies, comparable to the limit of detection of conventional thermocycling.

3.4 Specificity of microfluidic consensus-degenerate PCR

To assess specificity of the 1 μL PMMA microchips, we amplified 10^6 starting copies, or 1.25 ng, of EBV template in the presence of 2.5 ng of host human DNA. For comparison, we amplified the same quantity of template and host in a 5 μL conventional PCR tube. The resulting electropherograms of the PCR products are shown in Fig. 7. Non-specific products and primer dimers are observable in the conventional, but not the microchip, amplification. Qualitatively, the microchip exhibits improved specificity.

4 Discussion

Low volumes (e.g., < 5μL) can be problematic with conventional, injection-molded, polypropylene PCR tubes (Nakane et al. 2001). Not only does it present the challenges of preventing evaporation and recovering the sample, we suspect surface-related inhibition might also play a greater role with decreasing volume. Our BSA passivation results substantiate this claim, with improved success rate, notably for starting copies of 10^4–10^6 with volumes of 2–3 μL (SA: V = 3.8–4.5). BSA also improves success with constant SA: V at limiting starting copies: we measured a limit of detection of ~5,000 starting copies without BSA, but 1,000 starting copies with BSA. With starting copies ranging from 5×10^2–5×10^5, none of the 1 μL reactions led to successful amplification, underscoring the importance of microfluidic devices for amplification of these volumes.

We acknowledge that the use of end-point detection to quantify yield is, at best, semi-quantitative. Real-time PCR provides a more reliable quantitative measurement (Arya et al. 2005) and has been implemented for related studies (Taylor et al. 1997; Gonzalez et al. 2007; Kolari et al. 2007) but was not possible with our thermocycling methods. The use of electrophoresis for end-point detection has been used by others to present the effects of material inhibition by reporting the ranges of yield (Kodzius et al. 2011). While we caution that our PCR yield measurements are best for relative trends, the Agilent Bioanalyzer results were consistent.

Experimentally we have attempted to systematically explore the effects of SA:V, substrate, and the use of surface passivation with BSA and mineral oil encapsulation in microfluidic PCR. Varying the SA:V from 0 to 5.7, we showed a decaying PCR yield with increasing SA:V in the absence of passivation. The capillary segments used have dimensions less than the diffusion distance, *d*, thus we observed strong dependency of yield on SA:V. PC and COC give similar results, and PMMA is the worst option amongst these three material

candidates since it fails at SA: V = 5.7, while COC and PC can work at this high SA:V. This conclusion is in agreement with the assessments found in the literature (Kodzius et al. 2011).

The yield at high SA:V (e.g., >3) is improved and stabilized by the addition of BSA, especially so when the sample is incubated with BSA before loading the reaction. This stabilization of yield makes PCR viable at SA:V as high as 5.7 for all substrates tested this work. However, we note that, as others have posited (Taylor et al. 1997), BSA effects can be deleterious. For example, the yield of the control reaction (50 μL in a PCR tube) in Fig. 5 was lower with the addition of BSA as compared to without, confirming the complexity of the effects of BSA on the reaction chemistry and wall interaction (Kreader 1996; Jeyachandran et al. 2009; Christensen et al. 2007).

We measured the effects of all four combinations of the presence or absence of oil and BSA on PCR yield in a PMMA microchamber with SA:V = 7.0 relative to a control reaction (50 μL in a PCR tube) with and without BSA. Comparable to our previous experiments at SA:V>3 using capillary segments in a PP tube, the addition of BSA to the microchamber at SA:V = 7.0 improves (in fact, enables) PCR at high SA:V in a PMMA device. Adding oil to the reaction has an interesting effect. It improves yield whether or not BSA in used and the greatest improvement is obtained when BSA is not used. This is consistent with our previous results at SA:V<3, when BSA reduced reaction yield. Since oil encapsulation performs the passivation function, BSA is not recommended.

The enhancing effect of mineral oil is a result of the coating it provides, effectively encapsulating the sample volume and preventing surface adsorption of polymerase. The improved performance resulting from the exclusion of BSA was surprising and indicates a trade off between its benefits of passivation in high SA:V environments and its minor PCR inhibition, at least when in the presence of another passivation agent. BSA concentration could have been the confounding issue when paired with oil passivation, since there was less surface area for BSA to adsorb to, resulting in a greater amount of free BSA in solution and a higher likelihood of interfering with the reaction. Regarding the modeling of the effect of oil, though some have observed adsorption at the oil/water interface (Angione et al. 2012) and surfactant chemistry is known to be critical for droplet microfluidics (need references), in this work we found that the oil passivation has a far less deleterious effect on PCR yield than direct reaction/polymer interface. Our electropherograms were unable to resolve the expected difference between oil/water and polypropylene/water. We therefore conclude that oil alone is the most optimal passivation method amongst the options studied in this work.

We have presented the first microfluidic consensus degenerate PCR with the amplification of EBV by pan herpes virus PCR. We have optimized this device and reaction conditions with the first reported use of oil encapsulation without fluid flow and the use of standard reagent concentrations, yielding a limit of detection comparable to conventional tubes, with 140 starting copies or 3×10^5 copies/mL regarded as the accepted sensitivity threshold for diagnostic purposes (Wagner et al. 2001). This device and method thus represents a reliable, low-volume, low-cost approach to consensus degenerate PCR compared to the state of the art.

Since specificity is one of the most important factors with regard to the official acceptance of novel PCR assays within the clinical diagnostic laboratory, we demonstrate comparison of detection of EBV in the presence of background human DNA between a conventional 5 μL PCR tube and the 1 μL microfluidic chip. The comparison shows greatly improved specificity for the microchip. The CDC commonly uses nested-PCR, or amplification of a subset of the original target in a second PCR amplification to improve specificity and sensitivity in conventional consensus degenerate PCR. The benefits of the microchip could obviate this step, further saving time and cost. We attribute the consistently improved specificity to the enhanced temperature uniformity achieved at the microscale, since amplification of non-specific products is symptomatic of annealing temperature accuracy errors.

In order for the molecular biology community to embrace new technologies such as microfluidic PCR, the sensitivity and specificity capabilities for the most challenging and relevant reactions must compare or exceed those of conventional techniques while offering an easy-to-use, low-cost system. We have demonstrated a microfluidic PCR approach informed by experimental characterization of the common problem of inhibition by surface adsorption and factors that affect it: substrate, duration, surface area-to-volume ratio, and passivation technique. From this, we have implemented optimal passivation for a 1 μL reaction volume in a polymer microchip that we fabricated, providing a 50× volume reduction compared to conventional methods with comparable or improved sensitivity and specificity. Unlike the many microfluidic PCR devices that require higher concentrations of polymerase, which is the most expensive PCR reagent, we maintain a conventional polymerase concentration of 0.025 U/μL to provide true cost reduction. The application of our microchip to the detection of Epstein Barr virus using consensus degenerate primers, as routinely used by the CDC Pathogen Discovery Program, Division of Viral Disease, and our demonstrated ability to operate at the same limit of detection and specificity as conventional methods, makes the case for the viability of our microchip, taking a step closer to massive reductions in the cost and labor involved in pathogen screening and countless other PCR applications.

Acknowledgments

We acknowledge funding by the NSF (CISE 1110947, EHR 0965945) as well as American Heart Association (10GRNT4430029), the Georgia Economic Development Association, the Wallace H. Coulter Foundation, Centers for Disease Control and Prevention (CDC), NSF National Nanotechnology Infrastructure Network (NNIN), and from Georgia Tech: Institute for Bioengineering and Biosciences Junior Faculty Award, Technology Fee Fund, Invention Studio, and the George W. Woodruff School of Mechanical Engineering. We would like to personally thank Jing Zhang at the CDC for timely sample preparation. This research was performed under an appointment to the Department of Homeland Security (DHS) Scholarship and Fellowship Program, administered by the Oak Ridge Institute for Science and Education (ORISE) through an interagency agreement between the U.S. Department of Energy (DOE) and DHS. ORISE is managed by Oak Ridge Associated Universities (ORAU) under DOE contract number DE-AC05-06OR23100. All opinions expressed in this paper are the authors' and do not necessarily reflect the policies and views of DHS, DOE, or ORAU/ORISE. The findings and conclusions in this report are those of the authors and do not necessarily represent the views of the Centers for Disease Control and Prevention.

References

Angione SL, Chauhan A, Tripathi A. Real-time droplet DNA amplification with a new tablet platform. Anal Chem. 2012; 84:2654–2661. [PubMed: 22320164]

Arya M, Shergill IS, Williamson M, Gommersall L, Arya N, Patel HRH. Basic principles of real-time quantitative PCR. Expert Rev Mol Diagn. 2005; 5:209–219. [PubMed: 15833050]

Assis OBG. Scanning electron microscopy study of protein immobilized on SIO2 Sol–gel surfaces. Braz J Chem Eng. 2003; 20:339–342.

Beer NR, Hindson BJ, Wheeler EK, Hall SB, Rose KA, Kennedy IM, Colston BW. On-chip, real-time, single-copy polymerase chain reaction in picoliter droplets. Anal Chem. 2012; 79:8471–8475. [PubMed: 17929880]

Belgrader P, Young S, Yuan B, Primeau M, Christel LA, Pourahmadi F, Northrup MA. A battery-powered notebook thermal cycler for rapid multiplex real-time PCR analysis. Anal Chem. 2001; 73:286–289. [PubMed: 11199979]

Beverung CJ, Radke CJ, Blanch HW. Protein adsorption at the oil/water interface: characterization of adsorption kinetics by dynamic interfacial tension measurements. Biophys Chem. 1999; 81:59–80. [PubMed: 10520251]

Cao Q, Mahalanabis M, Chang J, Carey B, Hsieh C, Stanley A, Odell CA, Mitchell P, Feldman J, Pollock NR, Klapperich CM. Microfluidic chip for molecular amplification of influenza A RNA in human respiratory specimens. PLoS One. 2012; 7:e33176. [PubMed: 22457740]

Christensen TB, Pedersen CM, Grondahl KG, Jensen TG, Sekulovic A, Bang DD, Wolff A. PCR biocompatibility of labon-a-chip and MEMS materials. J Micromech Microeng. 2007; 17:1527–1532.

Dahl A, Sultan M, Jung A, Schwartz R, Lange M, Steinwand M, Livak KJ, Lehrach H, Nyarsik L. Quantitative PCR based expression analysis on a nanoliter scale using polymer nanowell chips. Biomed Microdevices. 2007; 9:307–314. [PubMed: 17203381]

Elbert DL, Hubbell JA. Surface Treatments of Polymers for Biocompatibility. Annu Rev Mater Sci. 1996; 26:365–294.

Erill I, Campoy S, Erill N, Barbe J, Aguilo J. Biochemical analysis and optimization of inhibition and adsorption phenomena in glasssilicon PCR-chips. Sensor Actuat B-Chem. 2003; 96:685–692.

Easley CJ, Karlinsey JM, Bienvenue JM, Legendre LA, Roper MG, Feldman SH, Hughes MA, Hewlett EL, Merkel TJ, Ferrance JP, Landers JP. A fully integrated microfluidic genetic analysis system with sample-in-answer-out capability. Proc Natl Acad Sci. 2006; 103:19272–19277. [PubMed: 17159153]

Focke M, Stumpf F, Faltin B, Reith P, Bamarni D, Wadle S, Muller C, Reinecke H, Schrenzel J, Francois P, Mark D, Roth G, Zengerle R, von Stetten F. Microstructuring of polymer films for sensitive genotyping by real-time PCR on a centrifugal microfluidic platform. Lab Chip. 2010; 10:2519–2526. [PubMed: 20607174]

Giordano BC, Copeland ER, Landers JP. Towards dynamic coating of glass microchip chambers for amplifying DNA via the polymerase chain reaction. Electrophoresis. 2001a; 22:334–340. [PubMed: 11288902]

Giordano BC, Ferrance JP, Swedberg S, Huhmer AFR, Landers JP. Polymerase chain reaction in polymeric microchips: DNA amplification in less than 240 s. Anal Biochem. 2001b; 291:124–132. [PubMed: 11262165]

Gonzalez A, Grimes R, Walsh E, Dalton T, Davies M. Interaction of quantitative PCR components with polymeric surfaces. Biomed Microdevices. 2007; 9:261–266. [PubMed: 17180709]

Gulley ML, Tang W. Using Epstein-Barr Viral Load Assays To Diagnose, Monitor, and Prevent Posttransplant Lymphoproliferative Disorder. Clin Microbiol Rev. 2010; 23:350–366. [PubMed: 20375356]

Haynes CA, Sliwinsky E, Norde W. Structural and Electrostatic Properties of Globular Proteins at a Polystyrene-Water Interface. J Colloid Interface Sci. 1994; 164:394–409.

Haynes CA, Norde W. Structures and Stabilities of Adsorbed Proteins. J Colloid Interface Sci. 1995; 169:313–328.

Hou CSJ, Godin M, Payer K, Chakrabarti R, Manalis SR. Integrated micro-electronic device for label-free nucleic acid amplification and detection. Lab Chip. 2007; 7:347–354. [PubMed: 17330166]

Hua Z, Rouse JL, Eckhardt AE, Srinivasan V, Pamula VK, Schell WA, Benton JL, Mitchell TG, Pollack MG. Multiplexed Real-Time Polymerase Chain Reaction on a Digital Microfluidic Platform. Anal Chem. 2010; 82:2310–2316. [PubMed: 20151681]

Jeyachandran YL, Mielczarski E, Rai B, Mielczarski JA. Quantitative and Qualitative Evaluation of Adsorption/Desorption of Bovine Serum Albumin on Hydrophilic and Hydrophobic Surfaces. Langmuir. 2009; 25:11614–11620. [PubMed: 19788219]

Kaur T, Singh J, Tong SX, Humphrey C, Clevenger D, Tan WD, Szekely B, Wang Y, Li Y, Alex Muse E, Kiyono M, Hanamura S, Inoue E, Nakamura M, Huffman MA, Jiang B, Nishida T. Descriptive epidemiology of fatal respiratory outbreaks and detection of a human-related metapneumovirus in wild chimpanzees (Pan troglodytes) at Mahale Mountains National Park, western Tanzania. Am J Primatol. 2008; 70:755–765. [PubMed: 18548512]

Kodzius R, Xiao K, Wu J, Yi X, Gong X, Foulds IG, Wen W. Inhibitory effect of common microfluidic materials on PCR outcome. Sensor Actuat B-Chem. 2011; 161:349–358.

Kolari K, Satokari R, Kataja K, Stenman J, Hokkanen A. Real-time analysis of PCR inhibition on microfluidic materials. Sensor Actuat B-Chem. 2007; 128:442–449.

Koutsopoulos S, van der Oost J, Norde W. Adsorption of an Endoglucanase from the Hyperthermophilic Pyrococcus furiosus on Hydrophobic (Polystyrene) and Hydrophilic (Silica) Surfaces Increases Protein Heat Stability. Langmuir. 2004; 20:6401–6406. [PubMed: 15248729]

Kreader CA. Relief of amplification inhibition in PCR with bovine serum albumin or T4 gene 32 protein. Appl Environ Microbiol. 1996; 62:1102–1106. [PubMed: 8975603]

Liu CN, Toriello NM, Mathies RA. Multichannel PCR-CE microdevice for genetic analysis. Anal Chem. 2006; 78:5474–5479. [PubMed: 16878885]

Liu P, Yeung SHI, Crenshaw KA, Crouse CA, Scherer JR, Mathies RA. Real-time forensic DNA analysis at a crime scene using a portable microchip analyzer. Forensic Science International: Genetics. 2008; 2:301–309. [PubMed: 19083840]

Liu Y, Rauch CB, Stevens RL, Lenigk R, Yang J, Rhine DB, Grodzinski P. DNA amplification and hybridization assays in integrated plastic monolithic devices. Anal Chem. 2012; 74:3063–3070. [PubMed: 12141665]

Louie M, Louie L, Simor AE. The role of DNA amplification technology in the diagnosis of infectious diseases. CMAJ. 2000; 163:301–309. [PubMed: 10951731]

Luk YY, Kato M, Mrksich M. Self-assembled Monolayers of Alkanethiolates presenting Mannitol groups are inert to protein adsorption and cell attachment. Langmuir. 2000; 16:9604–9608.

Martinez OM, de Gruijl FR. Molecular and immunologic mechanisms of cancer pathogenesis in solid organ transplant recipients. Am J Transplant. 2008; 8:2205–2211. [PubMed: 18801025]

Moskovitz Y, Srebnik S. Mean-Field Model of Immobilized Enzymes Embedded in a Grafted Polymer Layer. Biophys J. 2005; 89:22–31. [PubMed: 15805165]

Nakane J, Broemeling D, Donaldson R, Marziali A, Willis TD, O'Keefe M, Davis RW. A method for parallel, automated, thermal cycling of submicroliter samples. Genome Res. 2001; 11:441–447. [PubMed: 11230168]

Noinville S, Revault M, Baron MH. Conformational changes of enzymes adsorbed at liquid- solid interface: Relevance to enzymatic activity. Biopolymers. 2002; 67:323–326. [PubMed: 12012458]

Norde W, Haynes CA. Reversibility and the mechanism of protein adsorption (. American Chemical Society, ACS Symposium Series. 1995:26–40.

Orasanu-Gourlay A, Bradley RH. Protein Adsorption by Basal Plane Graphite Surfaces: Molecular Images and Nano-structured Films. Adsorpt Sci Technol. 2006; 24:117–130.

Pak N, Saunders DC, Phaneuf CR, Forest CR. Plug-and-play infrared laser-mediated PCR in a microfluidic chip. Biomed Microdevices. 2012; 14:427–433. [PubMed: 22218821]

Panaro NJ, Lou XJ, Fortina P, Kricka LJ, Wilding P. Surface Effects on PCR Reactions in Multichip Microfluidic Platforms. Biomed Microdevices. 2004; 6:75–80. [PubMed: 15307448]

Pancera SM, Petri DFS. Formation of enzymatic biofilms on polymer films and on silicon wafers. Mol Cryst Liq Cryst. 2002; 374:611–616.

Phaneuf, CR.; Forest, CR. Direct, High-Speed Milling of Polymer Microchamber Arrays. Proceedings of the 25th Annual Meeting of the American Society for Precision Engineering; Atlanta, GA. 2010. p. 345-347.

Prakash A, Amrein M, Kaler K. Characteristics and impact of Taq enzyme adsorption on surfaces in microfluidic devices. Microfluid Nanofluid. 2008; 4:295–305.

Rose TM, Schultz ER, Henikoff JG, Pietrokovski S, McCallum CM, Henikoff S. Consensus-degenerate hybrid oligonucleotide primers for amplification of distantly related sequences. Nucleic Acids Res. 1998; 26:1628–1635. [PubMed: 9512532]

Rose TM, Henikoff JG, Henikoff S. CODEHOP (COnsensus-DEgenerate Hybrid Oligonucleotide Primer) PCR primer design. Nucleic Acids Res. 2003; 31:3763–3766. [PubMed: 12824413]

Rose TM, Strand KB, Schultz ER, Schaefer G, Rankin GW, Thouless ME, Tsai CC, Bosch ML. Identification of two homologs of the Kaposi's sarcoma-associated herpesvirus (human herpesvirus 8) in retroperitoneal fibromatosis of different macaque species. J Virol. 1997; 71:4138–4144. [PubMed: 9094697]

Salas-Solano O, Ruiz-Martinez MC, Carrilho E, Kotler L, Karger BL. A sample purification method for rugged and highperformance DNA sequencing by capillary electrophoresis using replaceable polymer solutions B Quantitative determination of the role of sample matrix components on sequencing analysis. Anal Chem. 1998; 70:1528–1535. [PubMed: 9569762]

Shoffner MA, Cheng J, Hvichia GE, Kricka LJ, Wilding P. Chip PCR I Surface Passivation of Microfabricated Silicon-Glass Chips for PCR. Nucleic Acids Res. 1996; 24:375–379. [PubMed: 8628665]

Snow AL, Martinez OM. Epstein-Barr Virus: Evasive Maneuvers in the Development of PTLD. Am J Transplant. 2007; 7:271–277. [PubMed: 17229074]

Sofia SJ, Premnath V, Merrill EW. Poly(ethylene oxide) Grafted to Silicon Surfaces: Grafting Density and Protein Adsorption. Macromolecules. 1998; 31:5059–5070. [PubMed: 9680446]

Sweryda-Krawiec B, Devaraj H, Jacob G, Hickman JJ. A New Interpretation of Serum Albumin Surface Passivation. Langmuir. 2004; 20:2054–2056. [PubMed: 15835649]

Taylor TB, Winn-Deen ES, Picozza E, Woudenberg TM, Albin M. Optimization of the performance of the polymerase chain reaction in silicon-based microstructures. Nucleic Acids Res. 1997; 25:3164–3168. [PubMed: 9224619]

Tong S, Chern SWW, Li Y, Pallansch MA, Anderson LJ. Sensitive and Broadly Reactive Reverse Transcription-PCR Assays To Detect Novel Paramyxoviruses. J Clin Microbiol. 2008; 46:2652–2658. [PubMed: 18579717]

Wagner HJ, Wessel M, Jabs W, Smets F, Fischer L, Offner G, Bucsky P. Patients At Risk for Development of Posttransplant Lymphoproliferative Disorder: Plasma Versus Peripheral Blood Mononuclear Cells As Material for Quantification of Epstein-Barr Viral Load By Using Real-Time Quantitative Polymerase Chain Reaction. Transplantation. 2001; 72:1012–1019. [PubMed: 11579293]

Wang F, Burns M. Performance of nanoliter-sized droplet-based microfluidic PCR. Biomed Microdevices. 2009; 11:1071–1080. [PubMed: 19479169]

Wittwer CT, Garling DJ. Rapid cycle DNA amplification: time and temperature optimization. Biotechniques. 1991; 10:76–83. [PubMed: 2003928]

Yang J, Liu Y, Rauch CB, Stevens RL, Liu RH, Lenigk R, Grodzinski P. High sensitivity PCR assay in plastic micro reactors. Lab Chip. 2002; 2:179–187. [PubMed: 15100807]

Yang S, Rothman RE. PCR-based diagnostics for infectious diseases: uses, limitations, and future applications in acute-care settings. Lancet Infect Dis. 2004; 4:337–348. [PubMed: 15172342]

Yeo SH, Choi CR, Jung D, Park HY. Investigation of protein adsorption using plasma treatment for protein chips. J Korean Phys Soc. 2006; 48:1325–1328.

Yoon JY, Garrell RL. Preventing Biomolecular Adsorption in Electrowetting-Based Biofluidic Chips. Anal Chem. 2003; 75:5097–5102. [PubMed: 27669630]

Yu X, Zhang D, Li T, Hao L, Li X. 3-D microarrays biochip for DNA amplification in polydimethylsiloxane (PDMS) elastomer. Sensor Actuat A-Phys, Selected Papers from the Pacific Rim Workshop on Transducers and Micro/Nano Technologies. 2003; 108:103–107.

Zhang C, Xu J, Ma W, Zheng W. PCR microfluidic devices for DNA amplification. Biotechnol Adv. 2006; 24:243–284. [PubMed: 16326063]

Zhang Y, Ozdemir P. Microfluidic DNA amplification - A review. Anal Chim Acta. 2009; 638:115–125. [PubMed: 19327449]

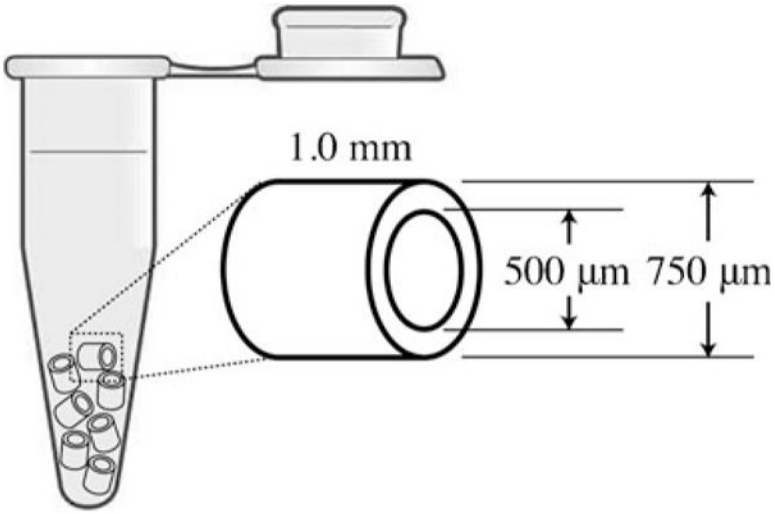

Fig. 1.

Within conventional PCR tubes, segments of polymer capillaries were submerged in 50 µL PCR reaction volumes to quantify the effect of SA:V and passivation on PCR yield.

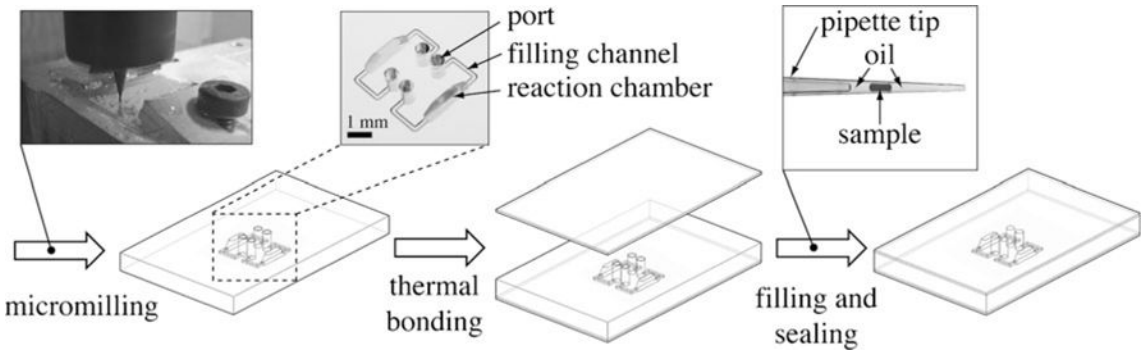

Fig. 2.

Polymer microchips were fabricated by micromilling 1 μL reaction chambers and filling channels into a PMMA substrate and encapsulating the features by thermal bonding then implemented by loading with a PCR sample using a standard micropipette and sealed with an adhesive film. SA:V = 7.0

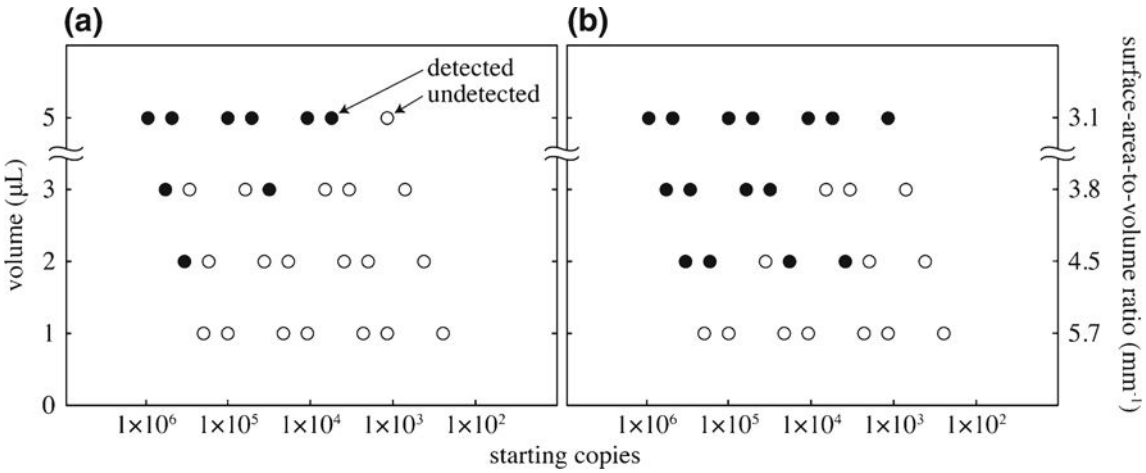

Fig. 3.

Epstein Barr virus detection results in conventional PCR tubes (**a**) without BSA and (**b**) with BSA for a range of starting copies. Filled circles indicate successfully detected samples and open circles indicate undetected samples. Reaction parameters: conventional PCR tubes, EBV template, BSA concentration 0.2 μg/μL, 40 cycles

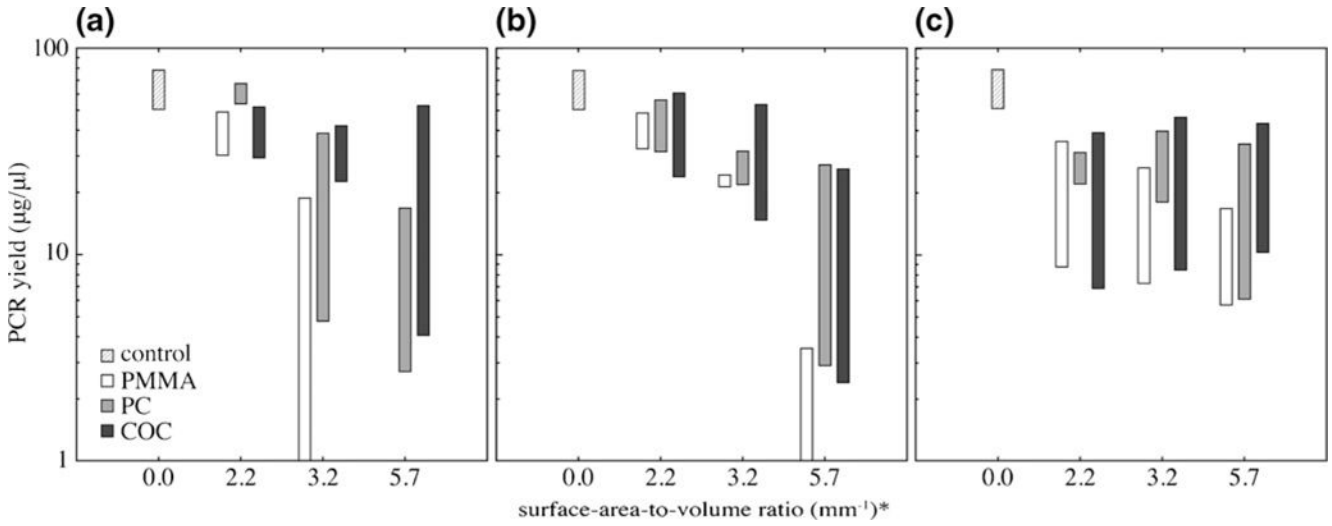

Fig. 4.

(**a**) Experimental PCR yield ranges in the presence of PMMA, PC, and COC capillary segments versus SA:V. (**b**, **c**) Effects of BSA passivation on PCR yield ranges when added to the PCR solution (**b**) immediately prior and (**c**) 12 h prior (overnight incubation) to thermocycling. Reaction parameters: conventional PCR tubes with capillary segments, 45.8 ng of λ-phage template, 30 cycles, 50 μL total volume, control has no segments, BSA concentration 0.2 μg/μL, n = 2. *Surface area of PP tube neglected as described in Section 2.3

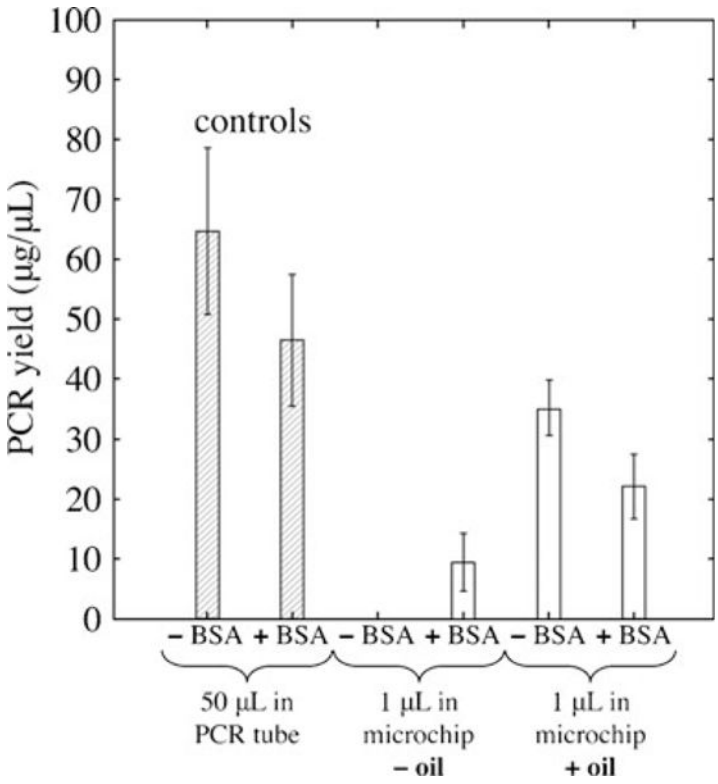

Fig. 5.

PCR yield for all combinations of mineral oil passivation and BSA passivation in PMMA microchips relative to control reactions in PCR tubes with and without BSA. Reaction parameters: control in conventional PCR tubes, microchips in PMMA with SA:V = 7.0, λ-phage template (45.8 ng in controls, 25 ng in microchips), 30 cycles, BSA concentration 0.3 μg/μL, n = 2

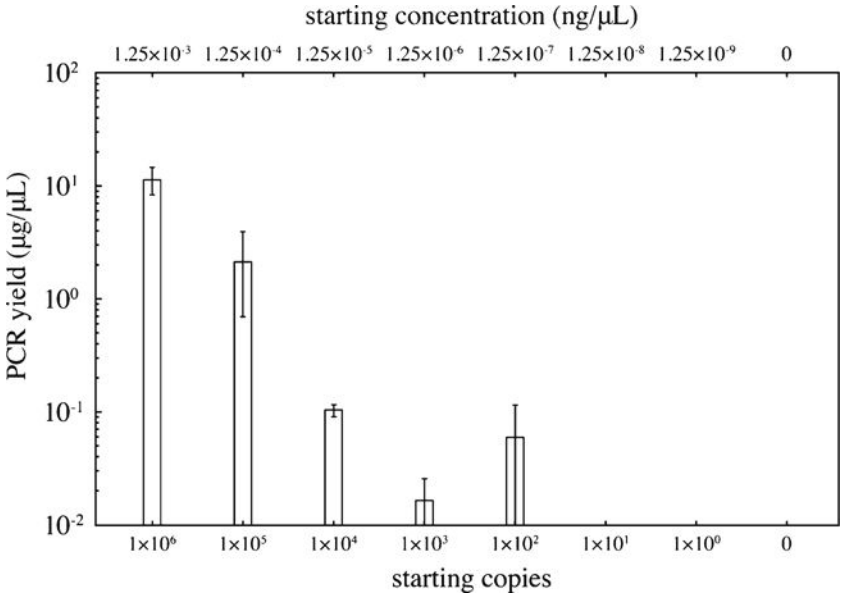

Fig. 6.

To assess sensitivity, PCR yield versus starting copies of Epstein Barr virus using 1 μL PMMA microchips with SA:V = 7.0. Limit of detection is 140 starting copies, equivalently 1.25×10^{-7}ng/μL or 3×10^{5} copies/mL. Reaction parameters: EBV template, 30 cycles, n = 3. Success rate was 100 % for 1.25×10^{-3}–1.25×10^{-5}ng/μL, and 66 % for 1.25×10^{-6}–1.25×10^{-7}ng/μL

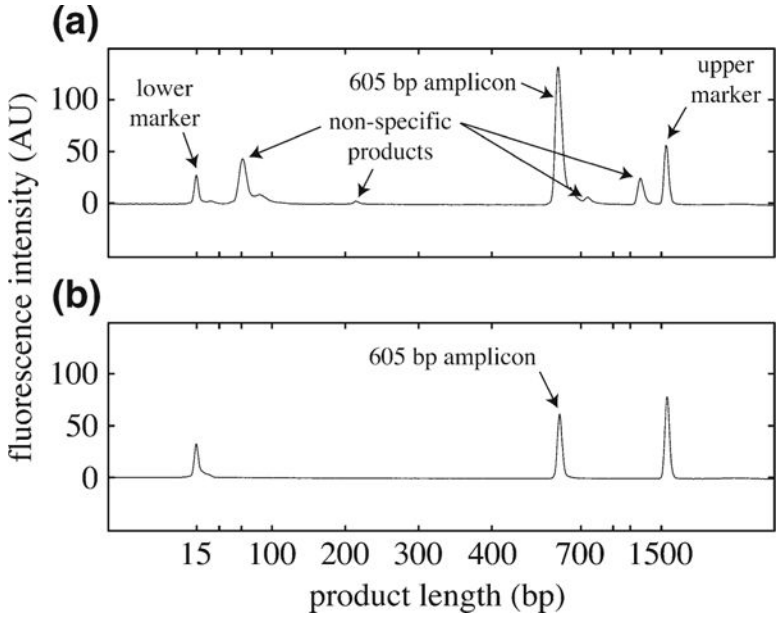

Fig. 7.

To assess specificity, electropherograms of PCR products and sizing markers for amplifications of 10^6 copies, or 1.25 ng, of Epstein Barr virus with 2.5 ng of background human DNA for (**a**) 5 μL reaction volumes in a conventional PCR tube and (**b**) 1 μL microchip. The target amplicon of 605 bp is detected in both, but the specificity (indicated by the presence of non-specific products) is superior for the microchip. One out of two identical results is shown. Reaction parameters: EBV template, 40 cycles